energy&fuels

Article

Comparisons on Formation Characteristics of NOx Precursors during Pyrolysis of Lignocellulosic Industrial Biomass Wastes

Hao Zhan, Xiuli Yin, Yanqin Huang, Hongyou Yuan,
Jianjun Xie, Chuangzhi Wu, Zhenxing Shen, and Jun-ji Cao

Just Accepted

ACS Publications

Comparisons on Formation Characteristics of NO$_x$ Precursors during Pyrolysis of Lignocellulosic Industrial Biomass Wastes

Hao Zhan[†,‡], Xiuli Yin[†], Yanqin Huang[†], Hongyou Yuan[†], Jianjun Xie[†], Chuangzhi Wu[†, *], Zhenxing Shen[ξ], and Junji Cao[**]

[†] *Key Laboratory of Renewable Energy, CAS, Guangdong Provincial Key Laboratory of New and Renewable Energy Research and Development, Guangzhou Institute of Energy Conversion, Chinese Academy of Sciences, Guangzhou 510640, People's Republic of China*

[‡] *University of Chinese Academy of Sciences, Beijing 100049, People's Republic of China*

[ξ] *Department of Environmental Sciences and Engineering, Xi'an Jiaotong University, Xi'an, 710049, People's Republic of China*

[**] *Key Lab of Aerosol Chemistry & Physics, Institute of Earth Environment, Chinese Academy of Sciences, Xi'an, 710045, People's Republic of China*

Abstract: Lignocellulosic industrial biomass wastes (IBWs) are dominant biomass resources in China while their thermal reutilization may bring serious environmental issues due to high nitrogen content. Investigation on the formation of NO$_x$ precursors during their pyrolysis is significant. Based on the pyrolysis of three typical ones - medium-density fiberboard waste (MFW), Chinese herb residue (CHR) and tea stalk waste (TSW) in a horizontal tubular quartz reactor, similarities and distinctions on the formation characteristics of NH$_3$ and HCN were investigated with the help of chemical absorption – spectrophotometry, XPS and TGA technologies. The results indicated that amide-N was the overwhelming nitrogen functionality in lignocellulosic IBWs, determining the dominance of NH$_3$ among NO$_x$ precursors. However, the ratio and total yield of HCN-N and NH$_3$-N could be changed by affecting intrinsic formation pathways owing to pyrolysis conditions as well as physicochemical properties. Joint effects of thermal conditions on each NO$_x$ precursor yield were sequenced as rapid pyrolysis at high temperatures > slow pyrolysis at high temperatures > rapid pyrolysis at low temperatures ≈ slow pyrolysis at low temperatures. Meanwhile, heating rate during slow pyrolysis had an ignorable impact. As a result, during rapid pyrolysis at high temperatures, larger particle size (0~900 μm) could significantly decrease the total yield by 16~17 *wt*% as well as favor NH$_3$-N yield, while both pyrolysis atmosphere and

1

moisture content presented limited effects. Furthermore, different thermal stability of amide-N type together with distinctive fuel components in three lignocellulosic IBWs led to their distinctions on the ratio of TSW > CHR > MFW at all temperature range and the total yield of MFW > CHR > TSW at low temperatures. However, total yield at high temperatures was observed at 20~45 *wt*%, which had no relationship with fuel types. These observations would provide some helpful guidance on clean thermal reutilization of lignocellulosic IBWs.

Keywords: Lignocellulosic IBWs; Amide-N; NO_x precursors; NH_3; Thermal stability

1. INTRODUCTION

With regard to biomass pyrolysis, besides converting biomass to bio-fuels with high grade heat in the absence of oxygen, it often occurs in gasification or combustion process when significantly less oxygen is provided than required for the stoichiometric coefficient.[1] During pyrolysis, fuel-bound nitrogen (Fuel-N) in biomass will be evolved into NO_x precursors such as NH_3, HCN and HNCO as well as the nitrogen in tar (Tar-N) and the nitrogen in char (Char-N). NO_x precursors can be converted into undesirable nitrogen-containing products including NO, N_2O and NO_2 during subsequent gasification or combustion. NO and NO_2 contribute to the formation of acid rain and photochemical smog. N_2O results in the enhancement of greenhouse effect and the destruction of stratospheric ozone layer.[2] Hence, to investigate the formation characteristics of NO_x precursors during biomass pyrolysis is significant for their thermal utilization.

Among biomass resources, industrial biomass wastes (IBWs) have been generally labeled as those with high organic matter that are mainly produced from light industry field, such as beverage production, wastewater treatment, food industries and pharmaceutical industries, etc. Statistics[3] suggest that the amount of IBWs from major light industrial process in China excesses 200 million tons per year. However, due to either the extrinsic introduction or the intrinsic existence for IBWs production, nitrogen content has been universally observed at a high level, such as coffee waste, soybean cake and fiberboard waste of 3~4 *wt*%[4,5], mycelia waste and sewage sludge of 6~8 *wt*%[6-8]. It is essential to investigate the formation of NO_x precursors during pyrolysis of these IBWs with high nitrogen content. As for NO_x precursors, HNCO is produced with a minor amount as well as

2

decomposed into HCN when pyrolysis temperature increases.[2] In addition, HNCO can be also hydrolyzed into NH_3 in wet

sampling systems according to the reaction: $HNCO + H_2O \rightarrow NH_3 + CO_2$.[4,7] Hence, NH_3 and HCN have been commonly

identified as the main species.

Up to now, some studies have been conducted on the formation of NO_x precursors during IBWs pyrolysis.[4-14] Their formation

pathways were briefly summarized as initial decomposition of Fuel-N and further conversion of Char-N/Tar-N formed in primary

reactions, which was correlated with pyrolysis conditions such as temperature, heating rate and pyrolysis atmosphere, and also

influenced by physicochemical properties of fuels referring to particle size, moisture content and fuel components. Among IBWs,

sewage sludge was the most common one widely investigated.[6-8,10-14] Some conclusions on the effects of pyrolysis conditions were

comprehensively obtained. NH_3-N yield (Y_{NH3-N}) and HCN-N yield (Y_{HCN-N}) showed an increasing tread in varying degrees with

the pyrolysis temperature for both slow and rapid pyrolysis.[6-8,11,14] However, it was proved that a certain amount of heterocyclic-N

(pyridinic-N, pyrrolic-N) were detected in raw sewage sludge besides the main protein-N structure[11,13,14], which was similar to that

in peat or low-rank coals.[15] Furthermore, it was also reported that hetero-aromatic structures would release nitrogen as HCN while

proteins (and/or amino acids) would mainly produce nitrogen as NH_3. Due to complex nitrogen functionalities in sewage sludge,

effects of pyrolysis conditions on the yields and dominant species of NO_x precursors were contradictable. Based on slow pyrolysis

under a similar condition, Y_{NH3-N} was observed in a great discrepancy of being far more than, equivalent to and less than Y_{HCN-N} in

studies of Tian et al.[6], Wei et al.[14], and Chen et al.[7], respectively. Based on rapid pyrolysis, some studies[8,11,12] proposed that NH_3

was the main one while HCN was observed to dominate in other studies[6,7,10]. Besides, during slow pyrolysis, Tian *et al.*[13] reported

that increasing heating rate would cause more rapid rise of both Y_{NH3-N} and Y_{HCN-N} for sewage sludge, which was totally in

contradiction with the result of de Jong *et al.*[16] focusing on some special biomass pyrolysis. As we know, there were many other

various IBWs produced from lignocellulosic biomass utilization besides sewage sludge. With regard to lignocellulosic biomass,

Hansson *et al.*[2] demonstrated that the majority of nitrogen in them was bound in proteins. It was inferred that nitrogen

functionalities in lignocellulosic IBWs were closer to that in conventional biomass compared with sewage sludge. Herein, a

variety of conclusions on sewage sludge couldn't fully reflect the characteristics of NO_x precursors for lignocellulosic IBWs. As

3

for these IBWs, Tian *et al.*[9] summarized the formation route of each NO_x precursor during cane trash pyrolysis. Becidan *et al.*[4] described the relationship between NO_x precursors and pyrolysis conditions for three high N-content IBWs. Yuan *et al.*[5] and Chen *et al.*[7] suggested that dominant species during pyrolysis of soybean cake and mycelia waste were NH_3 and HCN, respectively. It seemed that different specific lignocellulosic IBWs might have their distinctive characteristics on the formation of NO_x precursors. However, based on lignocellulosic IBWs with relevant nitrogen functionalities, there was still a lack of knowledge about similarities and discrepancies on the formation characteristics of NO_x precursors during their pyrolysis. Comparisons on the characteristic of each NO_x precursor produced therefore needed to be further explored.

In addition, it was mentioned that some physicochemical properties of conventional biomass would be partly correlated with the conversion of Fuel-N during their pyrolysis or gasification. Ren et al.[17] studied the effect of particle size on the formation of NO_x precursors during wheat straw pyrolysis. The result showed that large size was helpful for the formation of NH_3 while small size favored HCN. Moreover, Liu et al[18] found that NH_3 concentration in biogas decreased with the increase of moisture content during biomass gasification. For example, an increase in moisture content from 10 to 30 *wt*% resulted in a decrease of NH_3 emission from 230 to 175 ppmv. Additionally, as for fuel's components, it was observed differently that the HCN/NH_3 ratio would either go up[19-21] or drop down[5] with the increase of H/N ratio in fuels. However, Hansson et al.[2] proposed that HCN/NH_3 ratio was not significantly correlated with the fuel's O/N ratio. It was also reported that the ash and ash components in fuels had diverse effects on the yield of each NO_x precursor during straw pyrolysis due to their catalytic performance[21,22]. Due to the distinctive requirement of production processes, most lignocellulosic IBWs had more complex physicochemical properties such as different shape forms, high moisture content and various fuel components compared with conventional biomass.[4,5,7,9] Subsequently, these particular physicochemical properties in lignocellulosic IBWs would be essential to the formation of NO_x precursors in their real thermal reutilization. However, investigations on these aspects were rarely witnessed before.

Focusing on the deficiencies of predecessors' work on lignocellulosic IBWs, the objective of this article was to fully identify the characteristics of NO_x precursors to acquire some consistent valuable information during their pyrolysis. A woody one - medium-density fiberboard waste (MFW), and two herbaceous ones - Chinese herb residue (CHR) and tea stalk waste (TSW)

4

were employed. With regard to the selection of target lignocellulosic IBWs, three convincing reasons on their similar

characteristics have been proposed: (1) They were typically originated from different industrial fields with huge amount of 3.2

(MFW), 12 (CHR) and 2 (TSW) million tons per year.[3,23] (2) All of them could be regarded as renewable energy sources due to

their abundant organic matters and excellent heating value.[24-26] Subsequently, they could be well-reutilized and converted into

high value-added byproducts by thermal-chemical processes.[24,27-30] (3) They were reported to contain a considerable amount of

nitrogen related to the extrinsic additives (resin for MFW[24,31]) or the intrinsic components (protein/amino acid for CHR[27,28],

protein/caffeine for TSW[26]). Hence, based on pyrolysis of three lignocellulosic IBWs, effects of both pyrolysis conditions and

physicochemical properties of fuels on the formation of NO_x precursors were discussed and compared in detail. Meanwhile,

similarities and distinctions on the characteristics of NO_x precursors during pyrolysis of these IBWs with similar nitrogen

functionalities were also summarized.

2. EXPERIMENTAL SECTION

2.1. Materials.

The samples of MFW, CHR and TSW investigated were provided by a furniture manufacture plant, a herbal-tea beverage

production company and a green-tea production enterprise in China, respectively. Prior to the use and analysis, necessary

pretreatments of samples were applied, which included crushing, sieving and drying in sequence to make sure the dry samples

with suitable particle size. The proximate, ultimate and N-component analyses of samples were presented in Table 1.

2.2. Apparatus and Procedure

The experimental system mainly consisted of a gas supplying system, a pyrolyzer and a sampling system. The detailed

schematic diagram was shown in Fig. 1. The carrier gas (e.g. Ar, N_2 and CO_2) with purity of 99.999% controlled by a mass flow

meter was used to provide a different inert atmosphere for pyrolysis. The pyrolyzer was a horizontal tubular quartz reactor of 44

mm in inner diameter and 1200 mm in length. It was heated by a horizontal electric furnace with a temperature controller

governing temperature and heating rate. The operating temperature was monitored by a *k*-type thermocouple inserted into the

5

reactor. The sampling system was directly connected with the reactor in a flexible seal way. The connection pipe was constantly

heated by an electrical heating belt to avoid tar condensation. To minimize the inaccuracy of NO_x precursors caused by their

condensation in solutions[7,32], tar was sampling by a cold trap immersed in ice/water mixture without organic solvent. Meanwhile,

NH_3 and HCN were absorbed by two sampling lines in parallel. The cold trap was maintaining at about 273.15 K controlled by

ice/water mixture to ensure the complete collection of tar. Four impingers arranged in series comprised each sampling line, the gas

flow of which was controlled by a three-way control value. For each group, The first and last one were kept empty to prevent

suck-back and remove moisture, respectively. The remaining two with the same bubbling absorber (100 mL) were used to trap

each NO_x precursor. The absorbing solutions for NH_3 and HCN were H_3BO_3 (5 g/L) and NaOH (0.2 mol/L), respectively. Finally,

clean pyrolysis gas after the sampling system was vented or collected for gas analysis if necessary. All experiments were carried

out based on the designated operational conditions shown briefly in Table 2.

During each slow pyrolysis, about 3 g of sample contained by a ceramic boat was firstly placed into the center of pyrolyzer and

then the desired carrier gas with a flow rate of 600 mL·min^{-1} was maintained at least 30 min to purge air out. After the flushing

period, carrier gas was adjusted to 400 mL·min^{-1}. And the heating system was started to heat up the pyrolyzer to desired final

temperature at pre-designated heating rate. The final temperature was then held for 30 min to ensure the completion of all

reactions. During each rapid pyrolysis, about 3 g of sample was loaded into a ceramic boat and then placed at the cold side of

quartz tube. A gas flow of carrier gas (400 mL·min^{-1}) was started to remove any air from the system and the pyrolyzer was heated

up to the selected final temperature. When the set reactor temperature was attained and the reactor had been flushed for at least 30

min, ceramic boat was rapidly pushed into pre-heated zone and kept for the same residence time as slow pyrolysis to ensure that

all pyrolysis products were completely generated.

At the end of each run, char remained in ceramic boat was collected, weighed and stored for further analysis. Other pyrolysis

products passed through sampling system and were separately collected. Firstly, tar retained in cold trap was firstly washed by

isopropanol and then retrieved by evaporating the isopropanol solvent with rotary evaporator. After the tar sampling, NH_3 and

HCN left in pyrolysis gas were collected in parallel sampling lines with the corresponding absorbing solutions, respectively. The

gas flow of two sampling lines were recorded by volumetric gas meter to help for the calculation of NH_3 and HCN in absorbing

solution.

After the experiment, based on standards of HJ 536-2009 and HJ 484-2009, concentrations of NH_4^+ and CN^- ion in each

absorber were quantified by spectrophotometric method using a water quality analyzer (DR2700, HACH, USA). Each experiment

was carried out three times under the same condition to ensure the reliability, and the standard deviation for all results were within

$\pm$ 5%. The amounts of NH_3-N and HCN-N could be calculated by the gas flow of sampling line and the corresponding ion

concentration. Yields of NO_x precursors were described as follows.

$$Y_{NH3-N} = \frac{14.01 \cdot c_1 \cdot V_1}{\left(Q_1/(Q_1+Q_2)\cdot 18.04 \cdot m_{Fuel-N}\right)} \quad (1)$$

$$Y_{HCN-N} = \frac{14.01 \cdot c_2 \cdot V_2}{\left(Q_2/(Q_1+Q_2)\cdot 26.02 \cdot m_{Fuel-N}\right)} \quad (2)$$

$$Y_{total} = Y_{NH3-N} + Y_{HCN-N} \quad (3) \qquad R_{HCN-N/NH3-N} = \frac{Y_{HCN-N}}{Y_{NH3-N}} \quad (4)$$

where Y_{NH3-N} and Y_{HCN-N} were percentage of NH_3-N and HCN-N from Fuel-N, respectively, *wt*%; Y_{total} was defined as total yield

of two NO_x precursors, *wt*%; $R_{HCN-N/NH3-N}$ was defined as ratio of HCN-N/NH3-N, 1; m_{Fuel-N} were nitrogen mass of feedstocks, mg;

c_1 and c_2 were concentrations of NH_4^+ and CN^- in absorbing solution, respectively, $mg\cdot L^{-1}$; V_1 and V_2 were volumes of the

corresponding absorbing solutions, respectively, mL; Q_1 and Q_2 were gas flow of sampling line for NH_3 and HCN, respectively,

$mL\cdot min^{-1}$.

Especially, based on several experiments with typical operational conditions, yields of Char-N and Tar-N were determined as

follows: mass of both char and tar were calculated by gravimetric method, and nitrogen content in char and tar were analyzed with

an elemental analyzer (Vario EL cube, Elementaranalyse, Germany).

In addition, thermogravimetric behaviors and nitrogen functionalities of raw samples were confirmed using a simultaneous

thermal analyzer (Q50, TA Instruments, USA) and a X-ray photoelectron spectromenter (ESCALAB 250Xi, Thermo VG

Scientific, UK), respectively. TGA was performed with the temperature range of 50 - 900 °C at the designated heating rate (15, 30,

and 80 $°C\cdot min^{-1}$) in argon atmosphere with a flow rate of 40 mL/min. XPS spectra were acquired at a constant pass energy of 30

eV and a step size of 0.1 eV, with a spot size of 500 μm in diameter and an electron takeoff angle of 90°, using a Al Kα (1486.68

eV) X-ray source operating at 150 W.

3. RESULTS AND DISCUSSION

3.1. Comparisons on the Characteristics of Lignocellulosic IBWs

Fig. 2A presents TG/DTG profiles of three lignocellulosic IBWs as a function of temperature with different heating rate. Predominant weight loss occurs at 220~500 °C for MFW and 200~550 °C for both CHR and TSW, respectively, which is attributed to initial degradation of hemicellulose and further degradation of lignin and cellulose.[24,27,29] Besides, both TG and DTG curves for each lignocellulosic IBW change very little with increasing heating rate except the slight movement towards a higher temperature caused by the delayed kinetics of decomposition[33], which reveals that heating rate is not an important factor for thermal degradation of lignocellulosic IBWs.

Based on the calibration of 284.6 eV to principal C 1s component and the following curve-fitting principles: a mixed Gaussian (70%) - Lorentzian (30%) line shape, a FWHM of 1.65 eV and a Shirley-type background, XPS nitrogen (1s) spectra of three lignocellulosic IBWs after the resolution were obtained in Fig. 2B. XPS-peak-differentiating curve at binding energy of 399.9 ± 0.2 eV almost coincides with the original signal curve. According to energy positions of relevant nitrogen functionalities: 398.8, 399.9, 400.4, 401.4 (± 0.2) and 402-405 eV (pyridinic-N, protein-N/amide-N/amine-N, pyrrolic-N, quaternary-N and N-oxide, respectively)[13,14,34], protein-N (amide-N or amine-N) may be suggested to be the nitrogen functionality in each IBW. And no hetero-aromatic nitrogen structures are detected in XPS spectra. Leppalahti et al.[15] indicated that nitrogen functionalities were transforming from pyridinic-N/pyrrolic-N to protein-N/amine-N with the increase of Fuel-O from coal to wood. Hansson et al.[2] mentioned that protein-N was the main nitrogen source in wood. Knicker et al.[35] demonstrated that 80-90% nitrogen was assigned to amide/peptide structures in herbaceous biomass. Subsequently, it is reasonable that one single peak is witnessed in each lignocellulosic IBW spectrum. According to the detected data in Table 1, polyamide, protein and protein/caffeine are found to be overwhelming nitrogen components for MFW, CHR and TSW, respectively. It is easy to know that both polyamide and protein are the polymerization forms of amide-N. Meanwhile, caffeine containing amide-N bond may be regarded as one of amide derivatives.

8

Furthermore, energy position of amide-N was indistinguishable from that of amine-N (protein-N)[34] and quite close to that of

caffeine (399.80 eV)[36] in XPS spectrums. Hence, the single XPS peak for each lignocellulosic IBW can be assigned as amide-N.

Based on proximate, ultimate, thermogravimetric and XPS analyses, distinctions on three lignocellulosic IBWs are summarized.

1) Compared with two herbaceous IBWs, temperature range of predominant weight loss for MFW is narrower due to its higher

volatile close to wood.[24] Meanwhile, reaction rate and temperature at DTG peak are also higher. Besides, an obvious shoulder

peak at 294~320 °C is observed in DTG curve of MFW due to decomposition of polyamide structure[31], demonstrating that

polyamide is the most labile amide-N type. 2) The discrepancy of binding energy on target XPS peak for MFW and CHR/TSW is

due to different nitrogen sources for the former (polyamide structure[4]) and the latter two (protein or caffeine[26,37]). Ash and

nitrogen content for three lignocellulosic IBWs are both distinctive, corresponding to overall weight loss in TG curve and peak

area in XPS spectra, respectively. 3) Comparing two herbaceous IBWs, both thermogravimetric behaviors and nitrogen

functionalities are considerably similar. Nevertheless, difference on ash component, ash content and nitrogen source are quite

obvious. Caffeine contributes to about 11.5% of total nitrogen for TSW besides main protein structures. In addition, it was proved

that abundant caffeine structure was found in bio-oil from low-temperature pyrolysis of coffee ground[38], indicating caffeine

containing both amide and heterocyclic C-N bonds is more thermally stable than protein.

3.2. The Formation of NO$_x$ Precursors with Pyrolysis Conditions

3.2.1.Effect of heating rate during slow pyrolysis. Heating rate during slow pyrolysis can determine the amount of pyrolysis

products.[1] To better understand the characteristics of NO$_x$ precursors during slow pyrolysis, based on pyrolysis temperature:

800 °C, atmosphere: Ar, particle size: 0~300 μm, moisture content: 0%, effect of heating rate on the formation of NO$_x$ precursors

was firstly confirmed. Fig. 3 gives the changes of Y_{NH3-N} and Y_{HCN-N} with heating rate during slow pyrolysis of three samples.

Y_{NH3-N} decreases by a certain amount while Y_{HCN-N} has an ignorable change with the increasing heating rate, which is obviously

different from the results of predecessors' work.[13,16] In addition, Y_{NH3-N} constantly behaves more predominant than Y_{HCN-N} when

pyrolyzing at any heating rate. It was well-known that secondary reactions of Tar-N/Char-N were responsible for the formation of

9

NO_x precursors when pyrolyzing at high temperatures.[2,10-13] In these secondary reactions, NH_3 was produced by decomposition of

primary amines, bimolecular reaction between imine and amine (in tars), and hydrogenation among heterocyclic-N, HCN and H

radicals (in chars), while HCN was mainly originated from thermal cracking of amine-N (in tars). Based on TG-DTG curves,

volatiles in lignocellulosic IBWs can be almost released below 550 °C. During slow pyrolysis, volatiles will be swept out of the

reactor instantly together with a relatively mild release when samples are heated slowly to a high final temperature. As a

consequence, secondary reactions of Tar-N can't have strongly responded when massive volatiles release (below 550 °C).

Meanwhile, the remaining volatiles and H radicals at high temperatures are limited. Hence, at high temperatures, the weak thermal

cracking of Tar-N during slow pyrolysis results in a small amount on Y_{HCN-N} with an ignorable fluctuation at different heating rate.

However, the relatively high Y_{NH3-N} may be due to NH_3 accumulation from the direct thermal decomposition of nitrogen

functionality in fuels during heating process. With the increase of heating rate, the shorter residence time of HCN and H radicals

with char will weaken hydrogenation reactions (the main formation pathway of NH_3 during slow pyrolysis at high temperatures[6]),

leading to a decrease on Y_{NH3-N}. However, the mild drop on Y_{NH3-N} and the minor fluctuation on Y_{HCN-N} have indicated that heating

rate does not play an important role in the formation of NO_x precursors, corresponding to the thermogravimetric behaviors

affected by heating rate. In addition, it was evident that the formation of each NO_x precursor strongly depended on nitrogen

functionalities in fuels.[2,19] The origins of NH_3 involved the depolymerization of protein-N (in fuels), the

deamination/decomposition/bimolecular reactions of amine-N (in tars) and the hydrogenation of heterocyclic-N (in chars) in

sequence with the increase of temperature during pyrolysis.[11,12,13] This demonstrated a fact that every formation pathway of NH_3

was strongly linked with the initial thermal conversion of Fuel-N. As a result, it can be inferred that the predominant position of

Y_{NH3-N} depends on the overwhelming amide-N observed in lignocellulosic IBWs, having no relationship with heating rate.

3.2.2.Characteristics of NO_x precursors during slow and rapid pyrolysis. Based on the above conclusion that the variation of

heating rate don't remarkably affect each NO_x precursor yield, 15 °C•min^{-1} is chosen as a fixed heating rate during slow pyrolysis.

Characteristics of NO_x precursors during slow and rapid pyrolysis of three samples were investigated and compared. Fig. 4

displays changes of Y_{NH3-N} and Y_{HCN-N} at the temperature range from 300 to 900 °C during both slow and rapid pyrolysis.

As Fig. 4 shows, NH_3 is the dominant NO_x precursor during both slow and rapid pyrolysis at almost any final temperature, which reveals that dominant species of NO_x precursors won't be related to thermal conditions but probably depend on nitrogen functionalities in fuels. However, each NO_x precursor yield is varied with different final temperature under two pyrolysis types. As for slow pyrolysis, Y_{HCN-N} is produced at an ignorable amount while Y_{NH3-N} keeps a relatively remarkable level at low temperatures (<500 °C). The reason for this phenomenon is that the direct decomposition of amide-N contributes to the formation of NH_3 while there is no formation pathway for HCN except the weak dehydrogenation of amine-N (from decomposition of amide-N) at this temperature range, which is similarly depicted during slow pyrolysis of sewage sludge.[13] With the increasing pyrolysis temperature, Fuel-N conversion into both NH_3 and HCN slowly increase. When temperature goes up above 800 °C, Y_{NH3-N} has a slight drop for all samples. In Section 3.2.1, it is mentioned that secondary reactions at high temperatures are main contributors to each NO_x precursor and the detailed routes have been summarized. It is apparent that increasing temperature can guarantee that these secondary reactions become more and more obvious and intense, which consequently leads to the rise of both Y_{NH3-N} and Y_{HCN-N}. The slow release rate of NH_3 and HCN during slow pyrolysis can be explained that both hydrogenation of heterocyclic-N (in chars) into NH_3 and thermal cracking of amine-N (in tars) into HCN[6,11] are largely restricted due to less volatiles and H radicals remained at high temperatures. In addition, the slight decrease on Y_{NH3-N} may be attributed that the decomposition of NH_3 by inverse ammonia synthesis reactions[5] has become stronger than the formation of NH_3 by hydrogenation reactions when temperature goes up high.

As for rapid pyrolysis, it is interesting to note that both Y_{NH3-N} and Y_{HCN-N} are basically identical with that of slow pyrolysis below 500 °C, indicating that pyrolysis type has no effect on the formation of NO_x precursors at low temperatures. This may be due to that the direct decomposition of Fuel-N to NO_x precursors is hardly correlated with pyrolysis type. When temperature increases from 500 to 900 °C, Y_{NH3-N} shows an increment of 21.0 *wt*%, 20.3 *wt*% and 18.2 *wt*% while Y_{HCN-N} presents an increment of 18.3 *wt*%, 23.5 *wt*% and 27.9 *wt*% for MFW, CHR and TSW, respectively. A more dramatic change on Y_{HCN-N} than Y_{NH3-N} is observed for two herbaceous IBWs, indicating that thermal cracking of amine-N is more prevailing than hydrogenation of

11

heterocyclic-N when pyrolyzing at high temperatures. This phenomena distinguished by the type of IBWs are in detail explained in the subsequent discussions (effect of fuel's components). In addition, it is observed that each NO_x precursor yield with rapid pyrolysis is much higher than that with slow pyrolysis at high temperatures. Tian et al.[11] mentioned that secondary cracking of Tar-N/Char-N were the major pathways for NH_3 and HCN, and the decomposition of intermediates contributed to above 80% of total productions. Higher temperature can provide more activation energies to accelerate reaction rate meanwhile rapid pyrolysis can guarantee more volatiles involved in secondary cracking reactions, which shall be responsible for the higher Y_{NH3-N} and Y_{HCN-N}. Moreover, there is no plateau or drop for Y_{NH3-N} above 800 °C compared with slow pyrolysis, indicating that the main formation pathway of NH_3 (hydrogenation reaction) is still more dominant than other consumption pathways of NH_3 due to the more intense secondary cracking reactions.

In sum, it is crucial to emphasize the conclusion that both pyrolysis type and temperature won't change the dominant species of NO_x precursors but play a joint role in each NO_x precursor yield for three lignocellulosic IBWs. Both Y_{NH3-N} and Y_{HCN-N} are less influenced by pyrolysis temperature and independent of pyrolysis type at low temperatures (<500 °C), while show great diversities at high temperatures (>500 °C) due to the different dominant secondary reactions affected by pyrolysis type and temperature. Hence, rapid pyrolysis at high temperatures was chosen for the following discussion.

3.2.3.Effect of pyrolysis atmosphere. Nitrogen is the most common inert atmosphere available for the investigation on the pyrolysis process.[28-30] In addition, carbon dioxide is often considered as the gasifying agent to investigate the *in-situ* gasification of pyrolysis char. Thus, atmosphere is another pyrolysis condition affecting the formation of NO_x precursors when served as carrier gas during biomass pyrolysis. The effects of different gas atmosphere on the formation of NO_x precursors were compared during rapid pyrolysis of lignocellulosic IBWs at 600~900°C. Changes of $R_{HCN-N/NH3-N}$ and Y_{total} vs. temperature in different atmosphere were depicted in Fig. 5.

Both $R_{HCN-N/NH3-N}$ and Y_{total} increase with the increase of pyrolysis temperature in N_2 or CO_2 atmosphere, suggesting that the higher temperature favors the production of HCN and promotes the conversion of Fuel-N into NO_x precursors, which is consistent

12

with that in Ar atmosphere discussed above.

　　Comparing N_2 and Ar atmosphere, two curves on $R_{HCN-N/NH3-N}$ vs. temperature are basically in coincidence for each IBW (See Fig 5A), which demonstrates that N_2 isn't capable of affecting the balance between NH_3 and HCN produced at high temperatures. In addition, Y_{total} in N_2 atmosphere has a smaller drop than that in Ar atmosphere (See Fig 5B). It is inferred that the presence of N_2 may slightly hinder the formation reactions of NO_x precursors related to N_2 in nitrogen chemistry.[18] Hence, the presence of N_2 won't promote the formation of NO_x precursors during lignocellulosic IBWs pyrolysis. This observation is also indirectly supported by the view of Stubenberger et $al.$[20] that the only relevant source for NO_x emissions was the conversion of Fuel-N during solid biomass combustion.

　　Compared with Ar, Y_{total} has an evident drop when pyrolyzing in CO_2 atmosphere(See Fig 5B), reflecting that the presence of CO_2 can suppress the production of both NH_3 and HCN. This is in accordance with the results found in amino acid pyrolysis under Ar/CO_2 atmosphere.[39] However, there are some distinctions on $R_{HCN-N/NH3-N}$ among lignocellulosic IBWs (See Fig 5A). As for TSW and MFW, $R_{HCN-N/NH3-N}$ curve in CO_2 atmosphere is initially beneath that in Ar atmosphere and then close to even beyond it with the increase of temperature. It was reported that the introduction of CO_2 could consume active N-sites that had the potential to form HCN in Ar atmosphere.[17] Thus, due to the relatively weaker secondary reactions at lower temperatures (600-700 °C), the formation of HCN (thermal cracking of amine-N) is not so prevailing. In this situation , it is deduced that the inhibition effect on HCN by CO_2 is more significant under a pure CO_2 atmosphere. Subsequently, the restraint of HCN is stronger than that of NH_3, which causes a lower $R_{HCN-N/NH3-N}$. On the contrary, at higher temperatures (700-800 °C), increasing temperature can provide more activation energies for the prevailing thermal cracking of amine-N to produce HCN and a more gasification-similar atmosphere for CO_2 to consume NH_3, leading to a remarkable increase on $R_{HCN-N/NH3-N}$. As for CHR, $R_{HCN-N/NH3-N}$ curve in CO_2 atmosphere is always maintaining above that in Ar atmosphere with the temperature. One possible explanation is that the presence of CO_2 may weaken the catalytic performance of ash components on the conversion of fuel-N into NH_3 due to enough high ash content in CHR.[40] In a word, CO_2 atmosphere can be partly inhibit the production of NO_x precursors during lignocellulosic IBWs pyrolysis.

13

3.3. The Formation of NO$_x$ Precursors with Physicochemical Properties of Fuels

Having different shapes, containing high moisture and including various ash components are typical characteristics of most lignocellulosic IBWs. It is significant for their clean reutilization to understand the characteristics of NO$_x$ precursors affected by these physicochemical properties. Hence, effects of physicochemical properties of fuels involving particle size, moisture content and fuel components on the formation of NO$_x$ precursors were subsequently investigated.

3.3.1.Effect of particle size. Based on a fixed rapid pyrolysis condition with temperature of 800 °C, atmosphere of Ar and moisture content of 0 %, effect of particle size on the conversion of Fuel-N into NO$_x$ precursors for three lignocellulosic IBWs were discussed. Changes of $R_{HCN-N/NH3-N}$ and Y_{total} vs. particle size are shown in Fig. 6.

During rapid pyrolysis of lignocellulosic IBWs, Y_{total} presents a similar remarkable decrement by 16~17 *wt*% when particle size increases from 0~300 μm to 600~900 μm (See Fig 6B). Meanwhile, $R_{HCN-N/NH3-N}$ also has an obvious drop, indicating that the conversion of Fuel-N into NO$_x$ precursors favours NH$_3$ with the increase of particle size (See Fig 6A). As is known, the devolatilization rate shall be improved with the reduction in particle size, which results in the release of more volatiles during rapid pyrolysis process.[41] Subsequently the chance for secondary reactions of Tar-N can be largely enhanced, promoting the production of both NH$_3$ and HCN. Thereby, small particle size is more favorable for Y_{total}. The conclusion on Y_{total} is in agreement with the study of Ren *et al.*[17] that focused on slow pyrolysis of wheat straw. However, the change of Y_{NH3-N} with the particle size is opposite. It was found that larger particle size during slow pyrolysis would lead to more NH$_3$ production and explained that this situation provided more chance of secondary reactions, and then influenced the selectivity of N-conversion. Two opposite conclusions on Y_{NH3-N} by particle size are both reasonable due to the main different influencing pathways of NH$_3$ under different pyrolysis types. In addition, the decrease on $R_{HCN-N/NH3-N}$ with the increasing particle size can be explained that longer gas residence time within the char pores in larger particles promotes the hydrogenation of HCN into NH$_3$. The similar phenomenon and explanation can be found elsewhere.[4,17] It is also deduced that the decline of Y_{HCN-N} is more dramatic than that of Y_{NH3-N} when particle size increases during rapid pyrolysis of lignocellulosic IBWs.

14

3.3.2.Effect of moisture content. During rapid pyrolysis with a fixed condition (T_{final}: 800 °C, atmosphere: Ar, particle size: 0~300 µm), effect of moisture content on the formation of NO_x precursors for three lignocellulosic IBWs were investigated. Changes of $R_{HCN-N/NH3-N}$ and Y_{total} vs. moisture content are illustrated in Fig. 7.

Characteristics of NO_x precursors with the moisture content show different trends among three lignocellulosic IBWs. When moisture increases from 0% to 20%, Y_{total} firstly has an obvious drop and then goes up continually for MFW and TSW while keeps a constant rise trend for CHR (See Fig. 7B). However, $R_{HCN-N/NH3-N}$ presents a mild change for each lignocellulosic IBW while has a slight drop from a wet state to a wetter state (See Fig. 7A). The above phenomena may be explained by the balance of two opposite effects caused by moisture content. On one hand, it is easy to understand that the presence of moisture will to some extent cause the temperature delay of reaction region due to the energy consumption for vaporization when sample is pushed into reactor. Compared with a dry sample, either lower temperature at target reaction time or shorter retention time at target temperature will make secondary reactions weaker under the same pyrolysis condition for a wet one. This is called as the inhibition effect. On the other hand, the self-gasification condition can be formed with the introduction of high moisture content during rapid pyrolysis. Meanwhile, additional H radicals can therefore be generated for this "self-gasification" of sample by H_2O as moisture.[9] Subsequently thermal cracking of volatiles under self-gasification condition and hydrogenation of Char-N by H radicals can be enhanced. This is labeled as the promotion effect. Therefore, it can be inferred that inhibition effect is more prevailing when sample varies from a dry state to a low wet state for both TSW and MFW, leading to the decrease on both NH_3 and HCN. However, no drop for CHR is probably due to that promotion effect is always stronger than inhibition effect by the interaction between high ash content and moisture under a self-gasification condition.[42] Meanwhile, the rise of Y_{total} for a wet sample with the increase of moisture content in Fig. 7B is attributed that the more dominant promotion effect results in the increase of HCN (thermal cracking of volatiles) and NH_3 (hydrogenation of Char-N), respectively. In addition, hydrogenation of Char-N seems more intensive than thermal cracking of volatiles. Thus, the drops on $R_{HCN-N/NH3-N}$ are observed in Fig. 7A. And the hydrolysis of HCN into NH_3 may also contribute to this phenomenon.

15

3.3.3.Effect of fuel components. As discussed above, characteristics of NO_x precursors affected by both pyrolysis conditions and some physicochemical properties have much in common, there are still some distinctions on that for each IBW with different amide-N type and particular fuel components. Based on Ar atmosphere, particle size of 0~300 μm and moisture content of 0 %, Changes of $R_{HCN-N/NH3-N}$ and Y_{total} during rapid pyrolysis of three lignocellulosic IBWs were compared. Meanwhile, yields of Char-N and Tar-N with the pyrolysis temperature were also presented (See Fig. 8).

Effects of pyrolysis temperature on both $R_{HCN-N/NH3-N}$ and Y_{total} can correspond to the phenomenon and explanation presented in Section 3.2.2. Making a comparison of three lignocellulosic IBWs, $R_{HCN-N/NH3-N}$ has a constant sequence of TSW > CHR > MFW at all temperature range (See Fig. 8A). As for Y_{total}, it is produced with sequence of MFW > CHR > TSW at low temperatures (< 500°C) while independent of fuel types at high temperatures (> 500°C) (See Fig. 8B). The observations can be explained by the difference of fuel's components among three lignocellulosic IBWs (referring to thermal stability of amide-N type, ash content, nitrogen content), and the detailed explanations are given as follows.

At low temperatures, Y_{NH3-N} mainly contributes to Y_{total} because Y_{HCN-N} is produced at a small amount with minor fluctuation. It is demonstrated above that the thermal stability of relevant amide-N types is sequenced as: caffeine > protein > polyamide. The highest Y_{NH3-N} for MFW is due to the direct decomposition of polyamide at low temperatures. Meanwhile, the highest Tar-N yield and the lowest Char-N yield are also observed (See Fig. 8C). It was reported that the maximum emission of NH_3 occurred around 300°C as well as most of HNCO emitted between 250 and 400°C during UF resin pyrolysis[31], corresponding to the higher Y_{NH3-N} at 300 °C. This can also explain the mild drop on Y_{total} from 300 to 400 °C. Besides, caffeine (more stable) in TSW will be directly released into tar phase without decomposition at low temperatures[38], resulting in a higher ratio of Tar-N/Char-N compared with CHR (See Fig. 8C). Subsequently, a lower Y_{NH3-N} for TSW is ascribed to the direct decomposition of less amide-N. And the lower nitrogen content in TSW may also contribute to this observation.[19] Hence, Y_{NH3-N} with sequence of MFW > CHR > TSW results in the changes of both $R_{HCN-N/NH3-N}$ and Y_{total} at low temperatures.

On one hand, thermal degradation of herbaceous IBWs have a wider temperature range than that of woody IBW, which causes

16

stronger secondary reactions at high temperatures. As a result, more intense thermal cracking of amine-N will form more HCN.

Compared with CHR, TSW contains more Tar-N that has a larger drop at high temperatures(See Fig. 8C). This is probably

attributed to the cracking of abundant caffeine remained in tar[38]. The ring-opening of this structure can cause a more dramatic

increase on Y_{HCN-N}. For instance, Y_{HCN-N} reaches up a high level even more than Y_{NH3-N} for TSW between about 860-900 °C (See

Fig 4C). Hence, Y_{HCN-N} is observed with sequence of TSW > CHR > MFW at high temperatures. On the other hand, NH_3 mainly

originates from hydrogenation reactions activated by H radicals besides direct decomposition of Fuel-N at high temperatures. The

highest Y_{NH3-N} for MFW may be attributed to the major accumulation effect caused by the easier cracking of polyamide[31] as well

as the minor hydrogenation effect related to the presence of possible N-sites. As for herbaceous IBWs, ash components are

important factors for the formation of NO_x precursors during rapid pyrolysis.[37] Zhou et al[22] proved that calcium and potassium

could promote Y_{NH3-N} and Y_{HCN-N}. Differently, iron could promote Y_{NH3-N} while suppress Y_{HCN-N}. Thereby, CHR with higher

amounts of ash and its components can result in a higher Y_{NH3-N} than TSW. The bigger drop on Char-N for CHR at high

temperatures can also support this view. Furthermore, it is more obvious that Y_{NH3-N} is influenced by higher ash content in CHR

under a gasification-similar or self-gasification condition[40,42], making the distinctive characteristics of NO_x precursors when

discussing the influence of CO_2 atmosphere or moisture content above. To summarize, the opposite sequences of Y_{NH3-N} and

Y_{HCN-N} for three lignocellulosic IBWs cause a constant sequence of $R_{HCN-N/NH3-N}$ and an almost equivalence of Y_{total} at high

temperatures. Besides, it is interesting to note that $R_{HCN-N/NH3-N}$ goes up with the increase of H/N ratio, which is consistent with the

results in early studies.[19-21]

3.4. Formation Characteristics of NO$_x$ Precursors during Pyrolysis of Lignocellulosic IBWs

Based on the above discussion, similarities and distinctions on the formation characteristics of NO_x precursors are summarized

(See Fig. 9). The $R_{HCN-N/NH3-N}$ value is less than 1 during three lignocellulosic IBWs pyrolysis under any pyrolysis conditions,

demonstrating the dominance of NH_3 among NO_x precursors, which tightly depends on amide-N in fuels. Both pyrolysis

conditions and physicochemical properties inevitably alter $R_{HCN-N/NH3-N}$ and Y_{total} in varying degrees by intrinsically influencing

17

either primary or secondary reactions. Joint effects of pyrolysis type and temperature on each NO_x precursor yield are classified: slow pyrolysis at $T_{low} \approx$ rapid pyrolysis at T_{low} < slow pyrolysis at T_{high} < rapid pyrolysis at T_{high}. Meanwhile, heating rate during slow pyrolysis has a minimal impact. As a consequence, at T_{high} with rapid pyrolysis, larger particle size (from 0~300 to 600~900 μm) can strikingly decrease Y_{total} by 16~17 wt% as well as be more favourable for Y_{NH3-N}. However, both pyrolysis atmosphere and moisture content behave limited effects. Also, some distinctions on the characteristics of NO_x precursors for each IBW are observed due to thermal stability of amide-N type and particular fuel components. Sequences in $R_{HCN-N/NH3-N}$ of TSW > CHR > MFW at all temperature range and Y_{total} of MFW > CHR > TSW at T_{low} during rapid pyrolyis are obtained. However, Y_{total} at T_{high} is observed at a range of 20~45 wt%, having no relationship with fuel types. The founding is in accordance with the previous results under similar pyrolysis conditions[4,8,10].

4. CONCLUSIONS

In order to acquire more information on the clean thermal reutilization of lignocellulosic IBWs, three typical types with high nitrogen content were introduced to investigate the formation of NO_x precursors during their pyrolysis. Similarities and distinctions on the characteristics of NH_3 and HCN were analyzed and compared. NH_3 was the more predominant NO_x precursor during lignocellulosic IBWs pyrolysis, depending on the overwhelming nitrogen functionality - amide-N. However, due to pyrolysis conditions as well as physicochemical properties, $R_{HCN-N/NH3-N}$ and Y_{total} could be changed by affecting intrinsic formation pathways. Both Y_{NH3-N} and Y_{HCN-N} had little changes with heating rate during slow pyrolysis, and mild equal variations for two pyrolysis types at low temperatures, while were greatly enhanced during rapid pyrolysis at high temperatures. Subsequently, under this situation, increase on particle size strikingly decreased Y_{total} by 16~17 wt% as well as favored Y_{NH3-N}. However, effects of both pyrolysis atmosphere and moisture content were restricted. Moreover, different thermal stability of amide-N type and particular fuel components in these IBWs resulted in their distinctions on $R_{HCN-N/NH3-N}$ of TSW > CHR > MFW at all temperature range and Y_{total} of MFW > CHR > TSW at low temperatures. But then Y_{total} at high temperatures was observed at 20~45 wt%, which is independent of fuel types. These observations could be helpful for the control of NO_x precursors formation

18

in thermal reutilization of lignocellulosic IBWs.

AUTHOR INFORMATION

Corresponding Author

* E-mail: wucz@ms.giec.ac.cn

Notes

The authors declare no competing financial interest.

ABBREVIATIONS

IBWs = industrial biomass wastes; MFW = medium-density fiberboard waste; CHR = Chinese herb residue; TSW = tea stalk waste; Y_{NH3-N} = NH$_3$-N yield; Y_{HCN-N} = HCN-N yield; Y_{total} = total yield of HCN-N and NH$_3$-N; $R_{HCN-N/NH3-N}$ = ratio of HCN-N and NH$_3$-N

REFERENCES

(1) Balat, M.; Balat, M.; Kirtay, E.; Balat, H. *Energ. Convers. Manage.* **2009,** 50(12), 3147-3157.

(2) Hansson, K. M.; Samuelsson, J.; Tullin, C.; Amand, L. E. *Combust. Flame.* **2004,** 137(3), 265-277.

(3) Xu, G.; Ji, W.; Liu, Z.; Wan, Y.; Zhang, X. *Chin. J. Process Eng.* (in Chin.) **2009**, 9(3), 618-624.

(4) Becidan, M.; Skreiberg, O.; Hustad, J. E. *Energy Fuels* **2007,** 21(2), 1173-1180.

(5) Yuan, S.; Zhou, Z.; Li, J.; Chen, X.; Wang, F. *Energy Fuels* **2010,** 24(11), 6166-6171.

(6) Tian, F.; Li, B.; Chen, Y.; Li, C. *Fuel* **2002,** 81(17), 2203-2208.

19

(7) Chen, H.; Wang, Y.; Xu, G.; Yoshikawa, K. *Energies* **2012,** 5(12), 5418-5438.

(8) Cao, J.; Li, L.; Morishita, K.; Xiao, X.; Zhao, X.; Wei, X.; Takarada, T. *Fuel* **2013,** 104, 1-6.

(9) Tian, F.; Yu, J.; Mckenzie, L. J.; Hayashi, J.; Chiba, T.; Li, C. *Fuel* **2005,** 84(4), 371-376.

(10) Chen, H.; Namioka, T.; Yoshikawa, K. *Appl. Energy* **2011,** 88(12), 5032-5041.

(11) Tian, Y.; Zhang, J.; Zuo, W.; Chen, L.; Cui, Y.; Tan, T. *Environ. Sci. Technol.* **2013,** 47(7), 3498-3505.

(12) Zhang, J.; Tian, Y.; Cui, Y; Zuo, W.; Tan, T. *Bioresource Technol.* **2013,** 132, 57-63.

(13) Tian, K.; Liu, W.; Qian, T.; Jiang, H.; Yu, H. *Environ. Sci. Technol.* **2014,** 48(18), 10888-10896.

(14) Wei, L.; Wen, L.; Yang, T.; Zhang, N. *Energy Fuels* **2015,** 29(8), 5088-5094.

(15) Leppalahti, J.; Koljonen, T. *Fuel Process. Technol.* **1995,** 43(1), 1-45.

(16) de Jong, W.; Di Nola, G.; Venneker, B. C. H.; Spliethoff, H.; Wojtowicz, M. A. *Fuel* **2007,** 86(15), 2367-2376.

(17) Ren, Q.; Zhao, C.; Wu, X.; Liang, C.; Chen, X.; Shen, J.; Wang, Z. *Fuel* **2010,** 89(5), 1064-1069.

(18) Liu, H.; Gibbs, B. M. *Fuel* **2003,** 82(13), 1591-1604.

(19) Leppalahti, J. *Fuel* **1995,** 74(9), 1363-1368.

(20) Stubenberger, G.; Scharler, R.; Zahirovic, S.; Obernberger, I. *Fuel* **2008,** 87(6), 793-806.

(21) Ren, Q.; Zhao, C.; Wu, X.; Liang, C.; Chen, X.; Shen, J.; Tang, G.; Wang, Z. *J. Anal. Appl. Pyrol.* **2009,** 85(1-2), 447-453.

(22) Zhou, J.; Gao, P.; Dong, C.; Yang, Y. *J. Fuel Chem. Technol.* **2015,** 43(12), 1427-1432.

(23) Zhang, F.; Zhang, J. *Chin. Forest Prod. Ind.* (in Chin.) **2012**, 39(2), 35-37,40.

(24) Girods, P.; Dufour, A.; Rogaurne, Y.; Rogaurne, C.; Zoulalian, A. *J. Anal. Appl. Pyrol.* **2008,** 81(1), 113-120.

(25) Tripathy, V.; Basak, B. B.; Varghese, T. S.; Saha, A. *Phytochem. Lett.* **2015,** 14, 67-78.

(26) Sharma, A.; Vivekanand, V.; Singh, R. P. *Bioresource Technol.* **2008,** 99(9), 3444-3450.

(27) Zeng, X.; Shao, R.; Wang, F.; Dong, P.; Yu, J.; Xu, G. *Bioresource Technol.* **2016,** 206, 93-98.

(28) Wang, P.; Zhan, S.; Yu, H.; Xue, X.; Zhang, X; Hong, N. *Environ. Pollut. Control* (in Chin.) **2010,** 32, 14-18, 56.

(29) Gurten, I. I.; Ozmak, M.; Yagmur, E.; Aktas, Z. *Biomass Bioenerg.* **2012,** 37, 73-81.

(30) Uzun, B. B.; Apaydin-Varol, E.; Ates, F.; Ozbay, N.; Putun, A. E. *Fuel* **2010,** 89(1), 176-184.

(31) Jiang, X.; Li, C.; Chi, Y.; Yan, J. *J. Hazard Mater.* **2010,** 173(1-3), 205-210.

(32) Aznar, M.; Anselmo, M. S.; Manya, J. J.; Murillo, M. B. *Energy Fuels* **2009,** 23, 3236-3245.

(33) Shie, J.; Chang, C.; Lin, J.; Wu, C.; Lee, D. *J. Chem. Technol. Biot.* **2000,** 75(6), 443-450.

(34) Kelemen, S. R.; Afeworki, M.; Gorbaty, M. L.; Kwiatek, P. J.; Sansone, M.; Walters, C. C.; Cohen, A. D. *Energy Fuels* **2006,** 20(2), 635-652.

(35) Knicker, H.; Ludemann, H. D. *Org. Geochem.* **1995,** 23(4), 329-341.

(36) Plekan, O.; Feyer, V.; Richter, R.; Moise, A.; Coreno, M.; Prince, K. C.; Zaytseva, I. L.; Moskovskaya, T. E.; Soshnikov, D.

Y.; Trofimov, A. B. *J. Phys. Chem.* **2012,** 116(23), 5653-5664.

(37) Zhan, H.; Yin, X.; Huang, Y.; Zhang, X.; Yuan, H.; Xie, J.; Wu, C. *J. Fuel Chem. Technol.* **2017,** 45(3), 279-288.

(38) Cho, D.; Lee, J.; Yoon, K.; Ok, Y. S.; Kwon, E. E.; Song, H. *Energ. Convers. Manage.* **2016,** 127, 437-442.

(39) Ren, Q.; Zhao, C. *Environ. Sci.Technol.* **2012,** 46(7), 4236-4240.

(40) Jeremias, M.; Pohorely, M.; Bode, P.; Skoblia, S.; Beno, Z.; Svoboda, K. *Fuel* **2014,** 117, 917-925.

(41) Beis, S. H.; Onay, O.; Kockar, O. M. *Renew. Energ.* **2002,** 26(1), 21-32.

(42) Tian, F.; Yu, J.; McKenzie, L. J.; Hayashi, J.; Li, C. *Fuel* **2006,** 85(10-11), 1411-1417.

Table captions

Table 1 Properties of lignocellulosic IBWs in this work

Table 2 Operational conditions chosen for experiments

Figure captions

Figure 1. Schematic diagram of the experimental system.

Figure 2. TG/DTG and XPS analyses of three samples: A-TG/DTG profiles with different heating rate, B-N 1s XPS spectra.

Figure 3. Y_{NH3-N} and Y_{HCN-N} vs. heating rate during slow pyrolysis of three samples

Figure 4. Y_{NH3-N} and Y_{HCN-N} at different final temperature during slow (15 °C•min^{-1}) and rapid pyrolysis of three samples: A-MFW,

B-CHR, C-TSW.

Figure 5. Effect of different atmosphere on the characteristics of NO$_x$ precursors during rapid pyrolysis: A-$R_{HCN-N/NH3-N}$, B-Y_{total}.

Figure 6. Effect of particle size on the characteristics of NO$_x$ precursors during rapid pyrolysis: A-$R_{HCN-N/NH3-N}$, B-Y_{total}.

Figure 7. Effect of moisture content on the characteristics of NO$_x$ precursors during rapid pyrolysis: A-$R_{HCN-N/NH3-N}$, B-Y_{total}.

Figure 8. Characteristics of NO$_x$ precursors (A-$R_{HCN-N/NH3-N}$, B-Y_{total}) and Char-N/Tar-N yield (C) vs. the temperature during rapid

pyrolysis of three lignocellulosic IBWs.

Figure 9. Formation characteristics of NO$_x$ precursors during lignocellulosic IBWs pyrolysis

Table 1

Properties of lignocellulosic IBWs in this work

Samples	Proximate analysis (*wt*%, *db*)			Ultimate analysis (*wt*%, *daf*)					N-component content analysis (%, *db*)[b]				
	V	FC	A	C	H	S	N	O^a	N_{fuel}	$N_{protein}$	$N_{polyamide}$	$N_{caffeine}$	N_{others}
MFW	81.50	17.98	0.52	46.49	6.14	0.00	3.24	44.13	3.11	0.12	2.99	/	/
CHR	67.71	15.63	16.66	51.14	6.80	0.18	3.37	38.51	2.50	2.42	/	/	0.08
TSW	73.71	22.06	4.23	50.41	6.58	0.07	1.94	41.00	2.00	1.62	/	0.23	0.15

Ash analysis (%)[c]

Samples	SiO_2	Al_2O_3	MgO	Na_2O	Fe_2O_3	P_2O_5	CaO	K_2O	TiO_2	ZnO	SrO
CHR	21.98	7.92	7.66	0.40	4.82	4.56	20.78	7.64	0.44	0.09	0.08
TSW	0.50	1.50	5.97	0.30	0.25	16.86	8.61	31.20	0.11	0.07	0.03

[a] by difference; [b] based on weight of nitrogen; [c] expressed as form of metal oxide.

Table 2

Operational conditions chosen for experiments

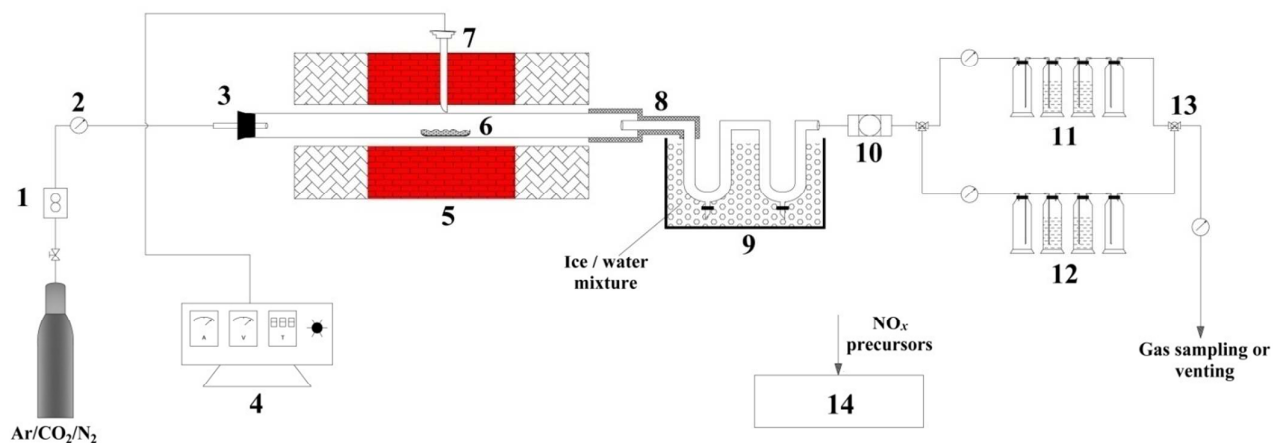| Conditions	Unit	Value range
pyrolysis type	$°C·min^{-1}$	slow pyrolysis: 15, 30, 80; rapid pyrolysis: $\sim10^3$
pyrolysis temperature	°C	from 300 to 900 with an interval of 100
pyrolysis atmosphere	/	Ar, N_2, CO_2
particle size	μm	0~300, 300~600, 600~900
moisture content	%	0, 5, 10, 15, 20

Fig. 1. Schematic diagram of the experimental system: 1-mass flow meter, 2-volumetric gas meter, 3-rubber plug, 4-temperature

controller, 5-horizontal tubular quartz reactor, 6-ceremic boat, 7-thermocouple, 8-electrical heating belt, 9-tar trap, 10-cotton filter,

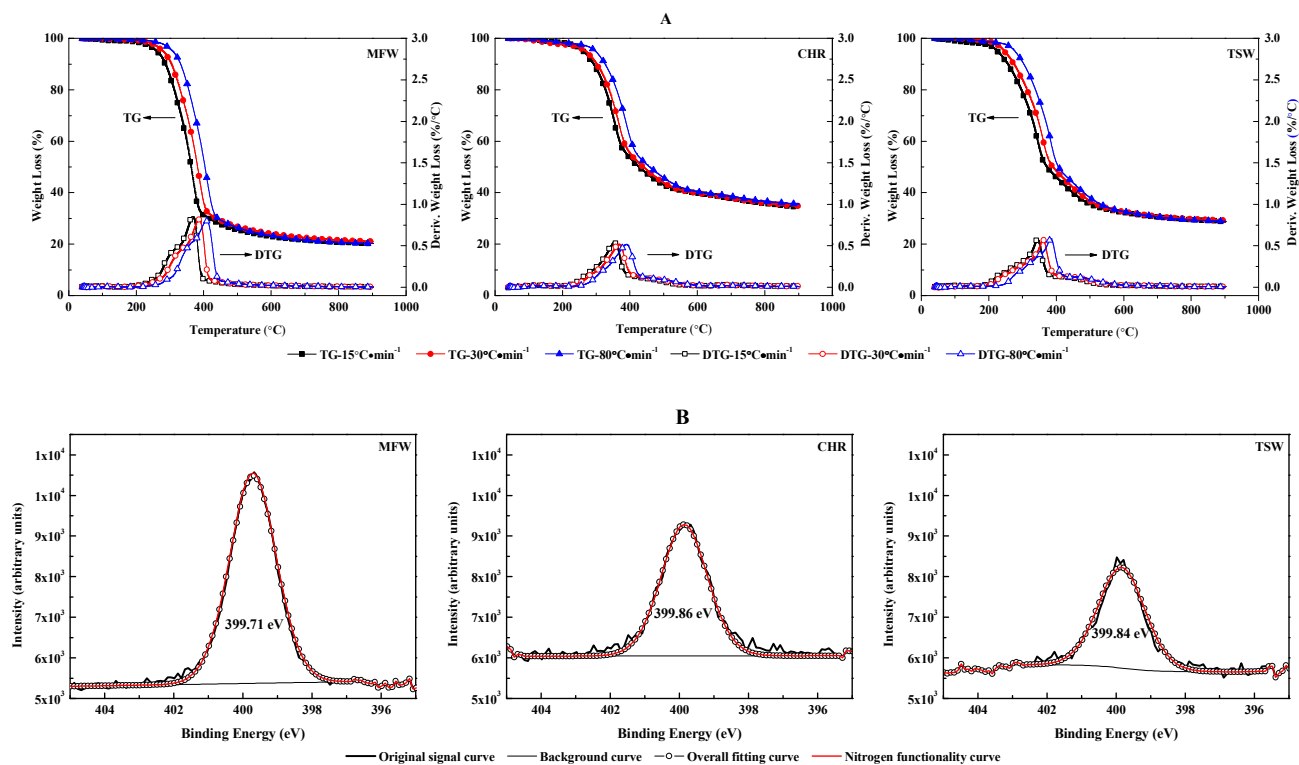11-HCN absorber, 12-NH$_3$ absorber, 13-three-way control value, 14-spectrophotometry

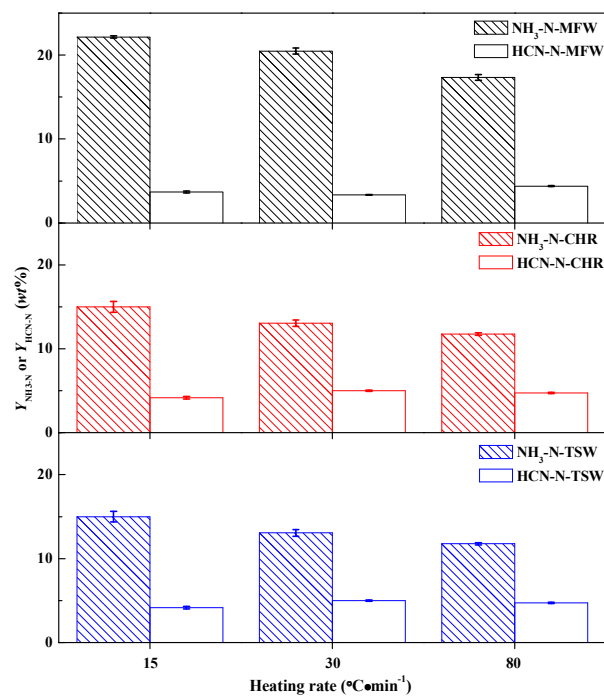**Fig. 2.** TG/DTG and XPS analyses of three samples: A-TG/DTG profiles with different heating rate, B-N 1s XPS spectra.

23

Fig. 3. Y_{NH3-N} and Y_{HCN-N} vs. heating rate during slow pyrolysis of three samples
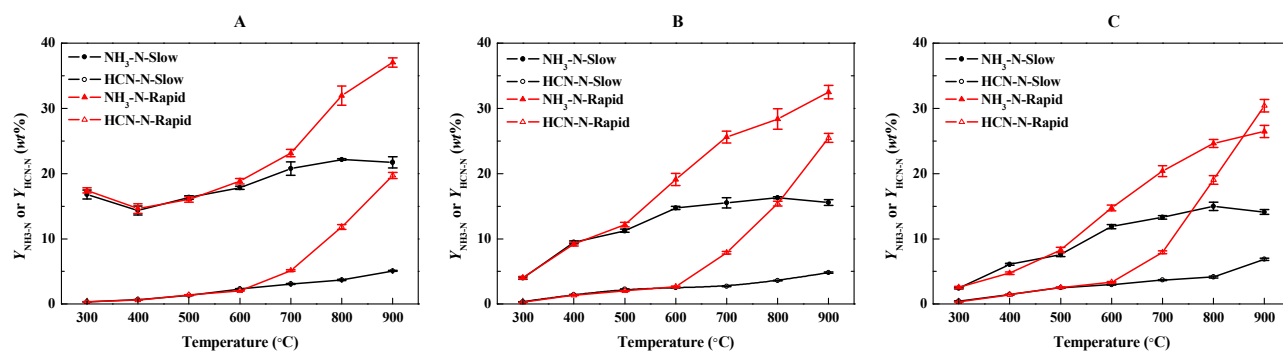
Fig. 4. Y_{NH3-N} and Y_{HCN-N} at different final temperature during slow (15 °C•min^{-1}) and rapid pyrolysis of three samples: A-MFW, B-CHR, C-TSW.

24

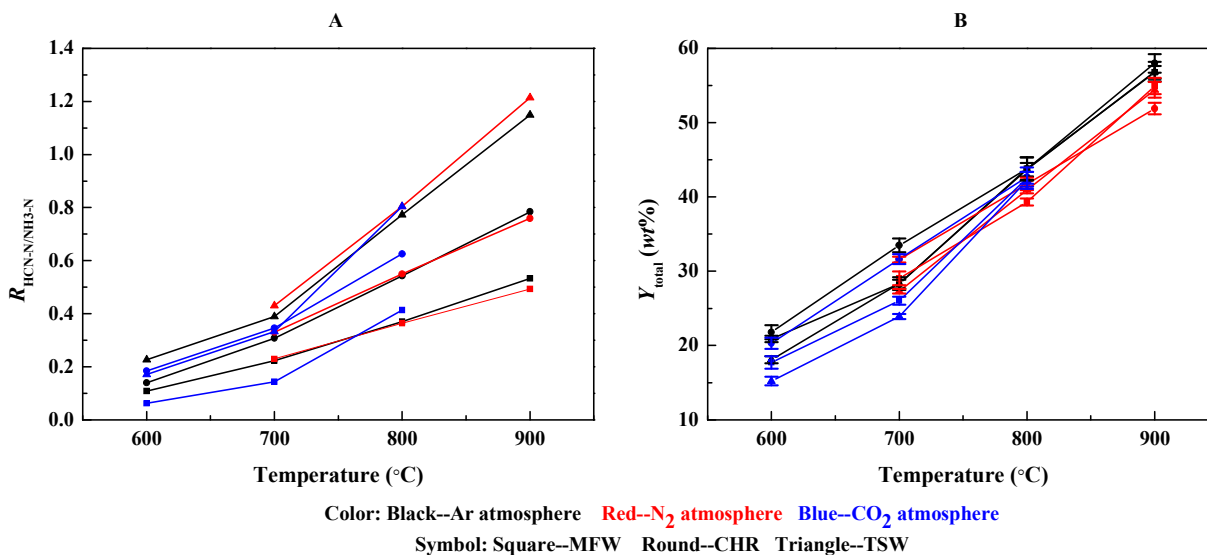Color: Black--Ar atmosphere   Red--N_2 atmosphere   Blue--CO_2 atmosphere

Symbol: Square--MFW   Round--CHR   Triangle--TSW

Fig. 5. Effect of different atmosphere on the characteristics of NO_x precursors during rapid pyrolysis: A-$R_{HCN-N/NH3-N}$, B-Y_{total}.
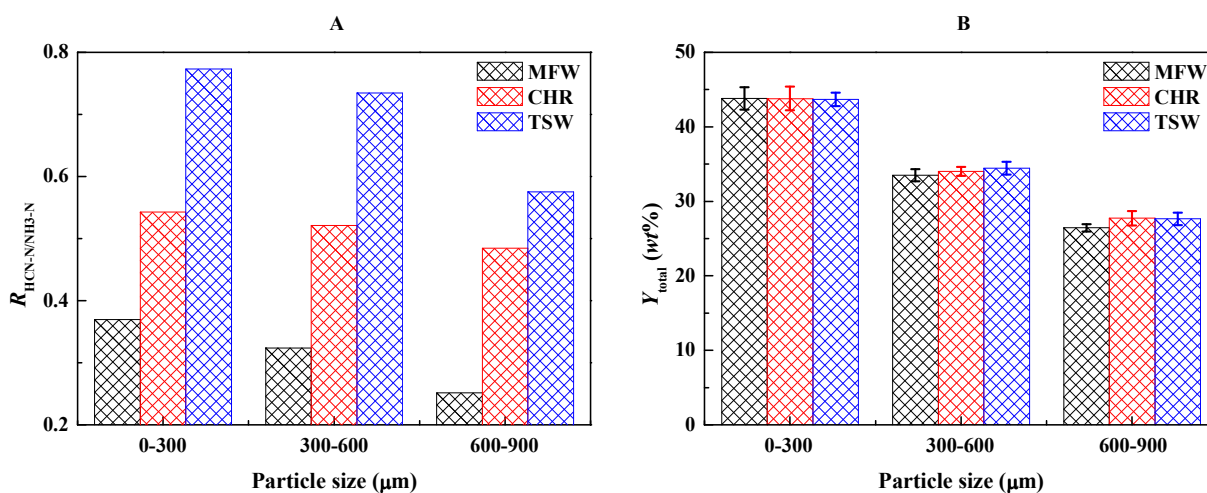
Fig. 6. Effect of particle size on the characteristics of NO_x precursors during rapid pyrolysis: A-$R_{HCN-N/NH3-N}$, B-Y_{total}.
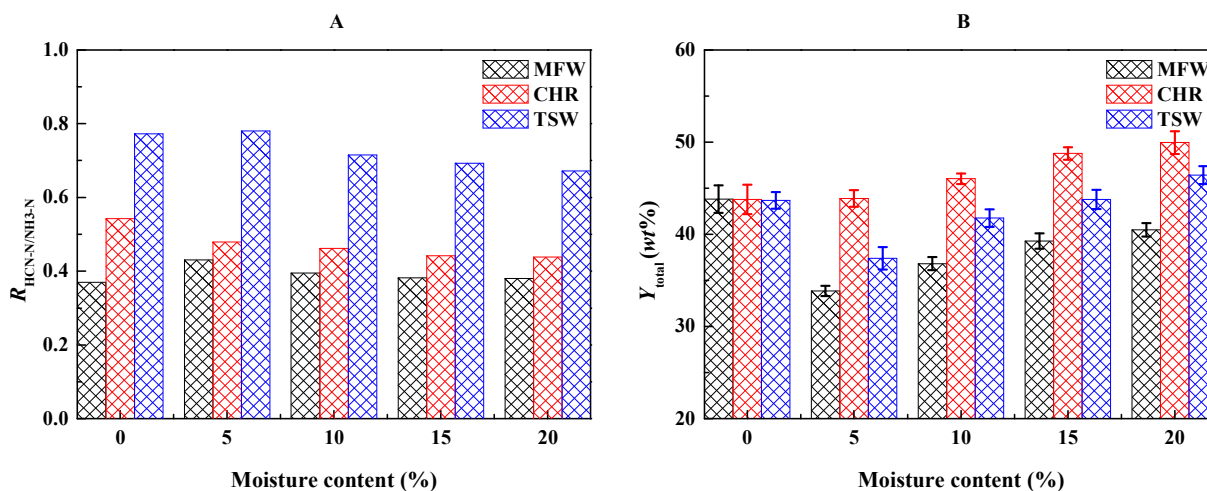
25

Fig. 7. Effect of moisture content on the characteristics of NO_x precursors during rapid pyrolysis: A-$R_{HCN-N/NH3-N}$, B-Y_{total}.

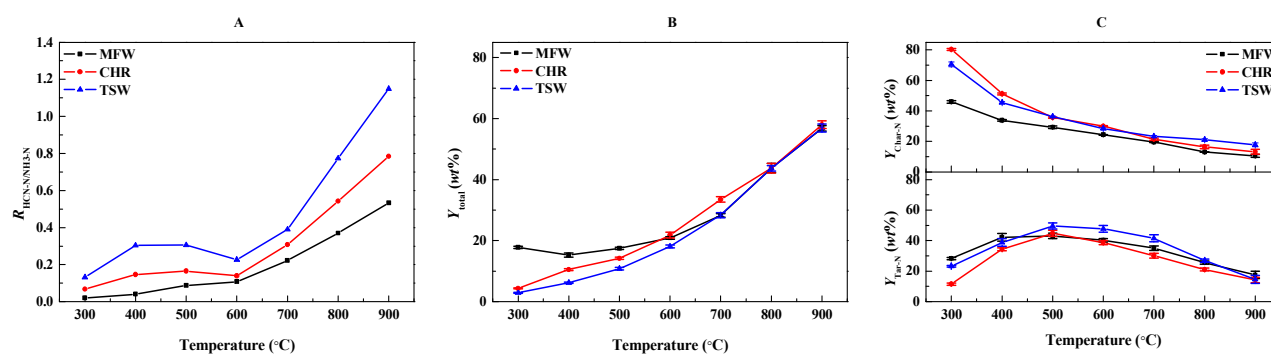**Fig. 8.** Characteristics of NO_x precursors (A-$R_{HCN-N/NH3-N}$, B-Y_{total}) and Char-N/Tar-N yield (C) vs. the temperature during rapid
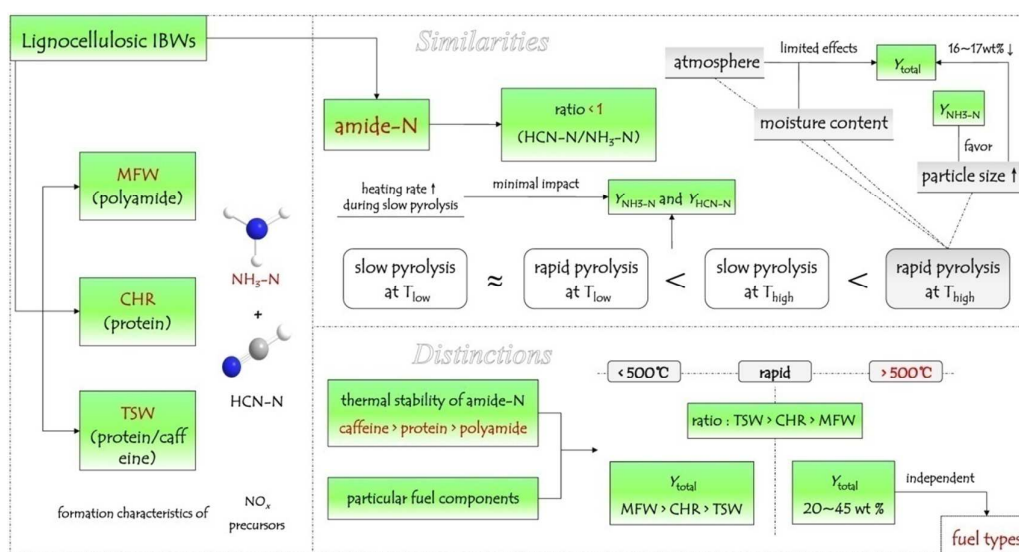
pyrolysis of three lignocellulosic IBWs.

Fig. 9. Formation characteristics of NO_x precursors during lignocellulosic IBWs pyrolysis

26